Lasers Manuf. Mater. Process. (2016) 3:141–157
DOI 10.1007/s40516-016-0027-6

High Efficiency Coupling of Optical Fibres with SU8 Micro-droplet Using Laser Welding Process

Seema Yardi[1,2,3] · **Ankur Gupta**[1,3] · **Poonam Sundriyal**[1,3] · **Geeta Bhatt**[1,3] · **Rishi Kant**[1,3] · **D. Boolchandani**[2] · **Shantanu Bhattacharya**[1,3]

Accepted: 15 April 2016 / Published online: 25 April 2016

Abstract Apart from micro- structure fabrication, ablation, lithography etc., lasers find a lot of utility in various areas like precision joining, device fabrication, local heat delivery for surface texturing and local change of microstructure fabrication of standalone optical micro-devices (like microspheres, micro-prisms, micro-scale ring resonators, optical switches etc). There is a wide utility of such systems in chemical/biochemical diagnostics and also communications where the standalone optical devices exist at a commercial scale but chip based devices with printed optics are necessary due to coupling issues between printed structures and external optics. This paper demonstrates a novel fabrication strategy used to join standalone optical fibres to microchip based printed optics using a simple SU8 drop. The fabrication process is deployed for fiber to fiber optical coupling and coupling between fiber and printed SU-8 waveguides. A CO_2 laser is used to locally heat the coupling made up of SU8 material. Optimization of various dimensional parameters using design of experiments (DOE) on the bonded assembly has been performed as a function of laser power, speed, cycle control, spot size so on so forth. Exclusive optical [RF] modelling has been performed to estimate the transmissibility of the optical fibers bonded to each other on a surface with SU8. Our studies indicate the formation of a Whispering gallery mode (WGM) across the micro-droplet leading to high transmissibility of the signal. Through this

Electronic supplementary material The online version of this article (doi:10.1007/s40516-016-0027-6) contains supplementary material, which is available to authorized users.

✉ Shantanu Bhattacharya
bhattacs@iitk.ac.in

[1] Microsystems Fabrication Laboratory, IIT Kanpur, Kanpur, India

[2] Electronics and Communication Engineering, MNIT, Jaipur 302017, India

[3] Mechanical Engineering, IIT, Kanpur 208016, India

work we have thus been able to develop a method of fabrication for optical coupling of standalone fibers or coupling of on-chip optics with off-chip illumination/detection.

Keywords SU8 · CO_2 laser · Laser welding · Waveguide coupling · Whispering gallery mode (WGM)

Introduction

The optical communication industry is rapidly progressing and changing from standalone structures like microspheres [1], micro prisms [2], ring resonators [3], optical switches [4] etc. to planar chip based Integrated Optical Systems (IOS). Among various performance measuring parameters in IOS, the transmittance highly depends on alignment and joining of the various components formulating such systems [5]. There are many applications of these IOS in fields of optical communication [6], optical sensing [7] and diagnostics for chemical/ biochemical analytes [8, 9], medical therapeutics [10] etc. The complexity and levels of engineering associated with realization of such systems have increased swiftly in the field of communication and sensing as stated by Moore's law [11]. In both cases multiple input/output signals are required to be handled in an environment on miniaturized chip based platforms. In most cases optical fibres are used for signal transmission purposes between such platforms and also formulate interconnect to off-chip optical signal readers, recorders (like spectrophotometer, intensity counter) etc. Similarly in the fields of biomedical diagnostics the lab-on-chip technology that is developed needs to be properly connected to reading/ recording instrumentation which are still off-chip and optically driven strategies of signal transmission from chip to reader are being heavily explored owing to the high speed of optical processes. While developing these interconnects, it is necessary that a strong bond is developed between the patterned structure in micro-chip architecture and the optical fibre so that they remain in position, without occupying much space on the IOS in order to carry out transmission of optical signals with minimum losses.

Previously, mathematical models [12, 13],experimental procedures [14] and computer simulation [15, 17, 20] of laser assisted bonding for various materials have been considered with variety of machining conditions. A range of work has been reported using SU8 material as a photo-resist for micro-fabrication of optical waveguides using spun thin films [16], but coupling of optical power to these systems is still a major problem. Apart from SU8 other alternate materials like ABS (Acrylonitrile Butadiene Styrene) [18], PMMA (Poly methyl methacrylate) and PC (poly carbonate) has shown good joining strength when exposed to laser source although their optical properties may not necessarily be commensurate to apply them for wave-guiding purposes in case of ABS and PC materials [19]. SU8 shows good absorption of UV light particularly below 350 nm but SU8 is transparent and insensitive to visible range and therefore may not be a suitable material of choice in the UV range. Another photopatternable polymer, Polynorbornene [21], although not widely available possesses similar T_g value as SU8 (≈215 °C) [21] and shows optical transparency to UV light (up to 239 nm). The polymer, Polynorbornene, however has been found to be quite brittle and therefore needs pretreatment to suitably adhere to substrates [22]. Various coupling strategies utilized for optical waveguide applications include usage of polystyrene microsphere

hybridized rib-like waveguides [23], optical solder as the gap filler in between the fiber and waveguide [24], vertically asymmetric design made up of a stepwise parabolically graded refractive index profile as combined with a horizontal taper in order to confine light in both directions [25] and miniature waveguide grating structure device on the end face of an optical fiber [26]. The methods so described are either complex in nature, involving phenomena like self assembly/ difficult micro-fabrication strategies or are accommodated outside the planar architecture of the IOC which is a fabrication challenge.

In the current work, SU8 photoresist with laser processing has been used as a contact bond material to facilitate a high coupling efficiency among chip bonded optical fibers. Low power CO_2 laser is used for stitching or welding of optical fiber to fiber using SU8 micro-droplet acting as a contact pad for the coupling and coupled ends of the optical transmitter. The coupling end of the transmitter is an off-chip fiber and the coupled end another spatially well located fiber on a microchip surface. The fiber coupled end is demonstrative of the whispering gallery mode formation which happens along the SU8 micro-droplet resulting in good transmissibility of input signal between the coupling (input) and the coupled (output) fiber. Both silicon and glass have been used as substrates for evaluating the efficacy of these contacts. Modeling of the heat transfer process has been undertaken by using COMSOL multi-physics version 4.3 and initial scanning speed/ power and other lasing parameters have been estimated before using them on the actual machine. A design of experiments (DOE) strategy has been put in place to further optimize the laser machining process. The SU8 micro-droplet joining both the fibers exhibit a whispering gallery mode (WGM) phenomenon along its circumference and with suitable positioning of fiber end with respect to the diameter of the microsphere it is able to transmit light between aligned and misaligned optical fibers with high efficacy. So in this manner we have been able to predict high transmittance couplings between self standing off chip fibers and printed optics.

Materials and Methods

SU8 photoresist polymer (M/S Micro chem. Inc.) is utilized as a bonding material for stitching optical fiber to Si or Glass substrates. The optical fibers are aligned using a clamping and positioning system over the substrate (Glass or Si) and a bead of SU8 2025 (M/S Microchem, Inc.), 1.05 μl in volume is dropped over the prior set optical fibers on the substrate. Laser heat treatment is done to firmly glue the two optical fibers to the substrate. The exact geometry of the drop is acheieved through an off-chip syringe pump dispensing the material and a prior modified surface of a certain surface energy so that the requisite contact angle of the drop on the surface is formulated. Experiments were carried out for misaligned and aligned fibers. (Fig. 1a and b) The Laser exposure has been carried out on EPILOG WIN32 laser machine with 32 W power and a total working platform of size 2 ft × 1 ft. The path of the Laser head was pre-programmed using Corel draw (Corel DRAW Graphics Suite X5) which was subsequently converted into a machine readable file of format '.dwf' and imported into the EPILOG machine. The laser parameters are fully optimized using DOE technique in which a Central Composite Design (CCD) is used to fit a model by least square technique. The software tool Software Design Expert 7.0, is used for this

purpose. After performing experiments, the images of fabricated designs were captured with top illuminated fluorescence microscope (Nikon 80i) in the bright-field mode. Transmittance of these welded pairs was measured using Ocean Optics Spectra Suite software, array detector [UV-VIS miniature fiber optic spectrometer] and a broadband [Halogen] light Source.

Mathematical Modeling and Simulation

The processing problem is multi disciplinary and involves Multiphysics considerations. In process modeling, finite element heat transfer model is used to find temperature distribution at the Air-fiber- SU8 interface and heat induced stress in the fiber. Using this information as input data in optical [RF] model, birefringence at the SU8 bonded fiber has been obtained.

Simulations Using COMSOL Multiphysics for Modeling the Whispering Gallery Mode (WGM)

The processing problem is multi disciplinary and involves Multiphysics considerations. In process modeling, finite element heat transfer model is used to find temperature distribution at the Air-fiber- SU8 interface and heat induced stress in the fiber. Using this information as input data in optical [RF] model, birefringence at the SU8 bonded fiber has been obtained.

All simulations have been carried out using an Intel (R) Core (TM) 2 Quad CPU, with 8.0 GB RAM and 64 bit operating system. The RF module of COMSOL multi-physics tool (version 4.4) was used for analyzing the patterned SU8 micro-drop bonding the standalone optical fiber to a polymeric waveguide. The governing equations that are used to model the whispering gallery modes from the Electro-magnetic wave frequency domain physics are the following:

$$\nabla \times \left(\mu_r^{-1} \nabla \times E\right) - K_0^2 \left(E_r - \frac{j\sigma}{\omega \varepsilon_0}\right) E = 0 \tag{1}$$

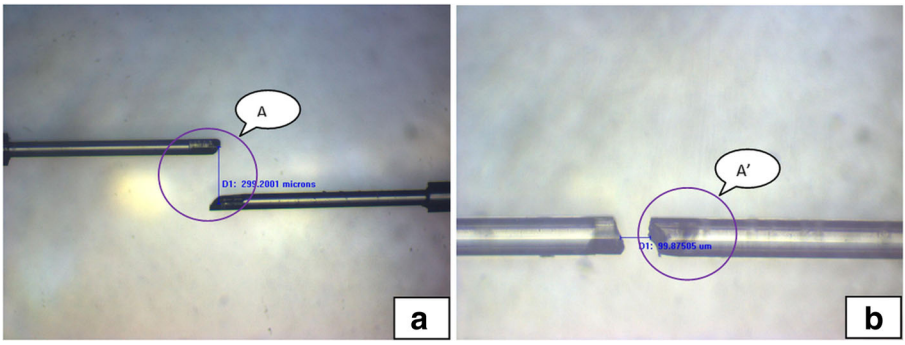

Fig. 1 **a** shows misaligned fibers to be connected by micro-droplet along the circumference A **b** Aligned fibers to be connected by micro-droplet along the circumference A'

$$\nabla \times \left(\mu_r^{-1} \nabla \times E\right) - K_0^2 \varepsilon_{rc} E = 0 \tag{2}$$

Where ε_r = (n-ik) ^{2} is relative permittivity [F/m] ('n' being the real part and 'k' being the complex part of the refractive index of the material (SU8 in our case), μ_r is relative permeability [H/m] both with respect to the permittivity and permeability of free space (ε_0 and μ_0 respectively) σ=conductivity [S/m], ω=angular frequency of the incident signal, K_0 is the wave number of free space represented by the following:

$$K_0 = \omega\sqrt{E_0\mu_0} = \frac{\omega}{c_0}\left[rad{\cdot}m^{-1}\right] \tag{3}$$

Where c_0 = Speed of light in vacuum [3×10^8 m/s].
Q-factor = f0/Δf is calculated from complex Eigen-frequency value W_r as

$$Q = \frac{R\varepsilon(W_r)}{2|1m(W_r)|} \tag{4}$$

Boundary conditions selected are perfect electric conductor [PEC], perfect magnetic conductor, electric field and domain condition is perfectly matched layer [PML] to control dispersive outer region.

Fabrication of Optical Interconnects Between Standalone Fibers and Patterned Waveguides

For performing fiber to fiber laser welding using SU8, four pairs of optical fibers are placed in close proximity on a glass slide, Si-wafer and Si/SiO_2 substrates. The distance between each individual pair is adjusted through Microscope. The interfaces are covered with small drops of SU8-2025. For fiber to SU8 waveguide laser welding through extended contacts, substrates (Glass, Si wafer) are spin coated with SU8-2025 with 1000 rpm at 30 s. Pre-baking was performed at 95° for 4–5 min followed by photo-lithography which was done using an M/S Union Optics mask alignment system. A second baking at 95 °C for 5 min was carried out to harden the photoresist. The substrates were developed for 2-3 mins in a suitable developer solution (M/S Microchem Inc.). The patterns generated were aligned under a microscope with the clamping and positioning system with respect to optical fibers and the SU8 micro-droplet was dispensed over the joint in volume of about [2.42E-10 m^3]0.242 micro-litre and . The SU8 micro-droplet was further stitched over the waveguide pattern on one end and the fiber on another end using the Epilog Laser Engraving Machine. The beam diameter of this machine is around 80 μm and the system emits at 10.6 μm wavelength. The laser path is designed using Corel Draw and is described to move the laser head over multiple droplets connecting the coupling to coupled fibers in a pre-designed layout. Each exposure of the laser is coincided with the geometric pole of the SU-8 micro-droplet and only a very small zone of the droplet is laser exposed. The laser power being highly focused in a small area guides the light past the whole radius of the micro-droplet all the way to the substrate over which the droplet is placed. The advantages of such laser welding processes are many including formulating a

strong joint between the optical fiber and substrate so that proper post aligned adherence levels can be achieved.

Figure 2a and b shows a schematic for an interconnect between two optical fibers across a Silicon substrate and an optical micrograph of an interconnected optical fiber on a substrate.

As the SU8 micro-droplet is top irradiated with laser, the heat transfer occurs across the surface of the droplet through its bulk to the substrate (Si or Glass) along a small polar region of the droplet. As discussed before depending on the heat transfer coefficient of the substrate if the heat is not conducted away by the substrates it can result in more localized heating although there is a chance of the droplet to totally melt and develop splashes. In this process the heat also flows across the embedded fiber thus melting and partially dissolving the fiber in SU8 so that on resolidification there is strong adherence between the substrate surface and the fiber. The softening of the optical fiber takes place at a temperature of 1600–1710 °C. DOE and number of tests carried out on Si and glass substrate for laser based bonding lead to optimized values of laser machine parameters. Images of fibre softening and fibre melting/ spill over are shown in Supplementary Information (Figure S1). The strength of the fiber weld after the laser heat delivery and resolidification time is qualitatively judged and categorized into four groups (Very Good, Good, Not Good and Bad) and further optical transmittance is found out. Optical fibre softening can be reached on Si or glass surface by controlling laser machine parameters as shown in Table 1.

Thermal direct bonding between the Silicon substrate and the optical fiber (without using SU-8) has also been attempted but the bond strength obtained was poor due to an unnecessary spill over of the fiber melt [Refer Supplementary Material Figure S1 (d)] and hence this option was ruled out. The fiber softening temperature is estimated to be in the higher range [1600–1710 °C] than SU8 so that there is no degradation of the fiber material or SU8 [600 ~ 900 K max] in the current study.

Method of Applying the Micro-droplet and the Method of Measurement of Transmittance Across the Coupling

After developing a strategy of coupling standalone fibers with the help of a SU8 micro-drop, it is important to test its efficacy and utility as a tool to extend optical signals from

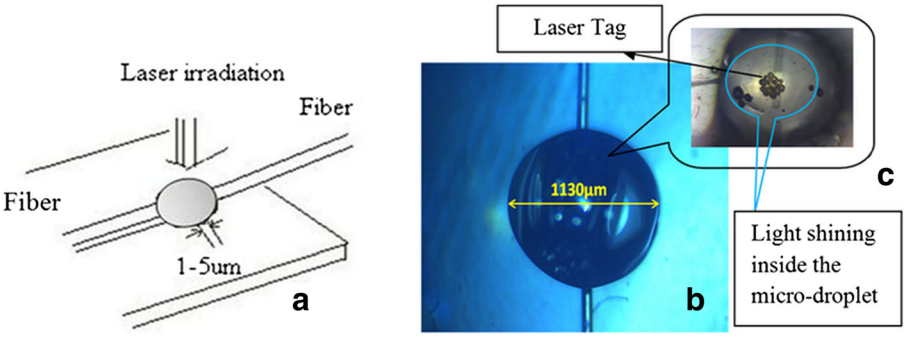

Fig. 2 **a** shows the schematic for a coupling between two optical fibers using the SU8 microdrop, **b** shows the optical micrograph of the micro-drop surface (*top elevation*) for the fiber/ fiber joint aligned case and **c** shows image of light shining inside a laser treated microdroplet

Table 1 Shows the percentage transmission obtained with variation in speed and power

S. No.	Corel draw pattern	% Power/ Speed	Weld strength	Optical transmittance
1.	Si + SU8 contact	100/1	Bad	–
2.		60/1	Good	0.00209
3.		50/1	Very good	0.744
4.		40/1	Good	0.09495
5.	Direct bonding of fiber on glass with no SU8 material	100/(40–80)	Good	–

light source to microchip and from microchip platform to measurement setup. Developed strategy may be extended easily to microchip based photo-patterned optical devices. The laser bonded fiber-waveguide-fiber and fiber-fiber assemblies were optically characterized for Transmittance measurement using Ocean Optics Spectrometer (Model Name: USB 4000 UV-VIS Miniature fiber optic Spectrometer, Spectra-Suite Software, Model No. USB4H02846 M/S Ocean Optics, Inc. Dunedin, FL 34698 with Halogen light source (HL-2000-HP-FHSA 034990459) and an integrated test setup was built for signal measurements.

Figure 3 shows the schematic diagram of the test set up. The Halogen lamp is a broadband light source [300–1100 nm] having peak measured value [R_λ] of 60,000 counts. As shown in this figure, two optical fibers are connected through a SU8 micro-drop which covers the fiber joint and bonds the fibers to a substrate wafer through laser heat. The micro-drop dispensing is performed by syringe pump which dispenses SU8 at a certain predetermined rate for a fixed time (to maintain droplet volume homogeneity) under a magnifying lens over pre-aligned fibers. The alignment process of the fiber is done using two precision XYZ stages. The first fiber is fixed on the substrate which is fixed and mounted over one of the XYZ stages. The other fiber is projected in space into the previously mounted glass substrate and is carried by a standalone holder placed near to the first XYZ stage. Once the fibers are aligned under the magnifying lens the second XYZ stage containing the syringe pump with a projected syringe is aligned first in the X-Y direction with respect to the coupling region and then the syringe pump is moved down in the – Z direction so that the droplet starts touching over the substrate.

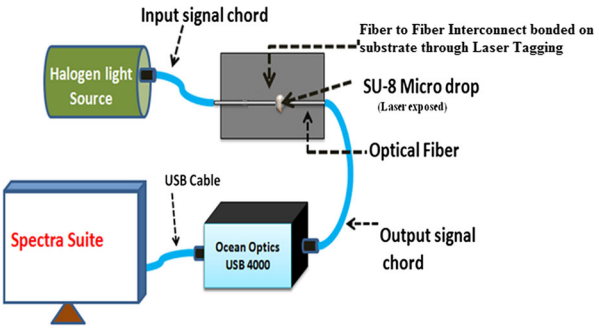

Fig. 3 Schematic diagram of test setup for measurement of transmittance

The droplet adheres to the substrate and the syringe is pulled back in the –X direction to release the droplet over the coupling region. Both XYZ stages are already calibrated for linear motion with respect to the rotational motion of the lead screw. This way the small distances between the aligned fibers for both the aligned and misaligned cases can be easily maintained. The drop volume is recorded as 1.05 μl and an accurate laser beam exposure of the exact location and spot-size in the polar region of the droplet can be obtained to ensure a perfect adherence of the spot and surrounding region to the substrate surface. SU8 grade 2025 has been found to offer the right viscosity to undertake this repeated dispensing. The substrate plays a major role in offering a relatively higher level of adhesion to the SU-8 drop and it de-adheres the drop from the needle body. Contact angle studies are made over the SU-8 droplet getting formulated over the silicon substrate and it is found that with a thermal grown oxide layer on surface the contact angle formulated by the droplet is approximately 76°[See figure S 2]. This method of fabrication ensures precision dispensing of SU8-2025 without affecting the surrounding miniaturized devices or structures. The output signal [$S_{O\lambda}$] is connected by optical fiber cable or chord to the Ocean optics USB4000 which is a UV-VIS miniature Fiber optical spectrometer. USB 4000 features 16 -bit A/D convertor, a set of CCD arrays, GPIOs, enhanced electronics and increased signal -to-noise ratio etc. It is connected to a computer system through an USB port and software named Spectra-Suite is used for spectroscopy with the advanced data capture attributes. It can control multiple USB devices monitored on the same graph independently. The output spectra has wavelength in 'nm' on X-axis and intensity (counts) on Y-axis. It suitably measures wavelength dependent transmittance of a sample or structure, absorbance, reflectance and relative irradiance. Before starting with the measurement reference [R_λ], dark [$D_{R\lambda}$] files referring to background subtraction must be acquired.

In order to ensure proper coupling efficiency the transmittance of an optical signal across such a coupling is numerically determined by percentage transmittance which represents the % amount of energy allowed to pass through a sample medium relative to energy passing through the reference medium.

$$\%\ \text{Transmittance} = \%\frac{S_{o\lambda}-D_{R\lambda}}{R_\lambda-D_{R\lambda}}\cdot 100 \tag{5}$$

Where $S_{o\lambda}$is signal output level, $D_{R\lambda}$ is dark reference signal level (Intensity = 1000 counts) and R_λ is a reference signal (taken as 60,000 counts in most cases). % Transmittance is ratio of two intensities hence it is unit-less quantity expressed as a %. After following procedural steps for transmittance measurement, a graph /spectra of wavelength dependent % transmittance is obtained on the active window of the Spectra Suite. The % transmittance is further measured in the aligned and mis-aligned cases for the micro-droplet.

Further, a comparison of absorptivity with and without SU8 on glass/ Si was made where; Absorptivity (ε) was measured at a given wavelength corresponding to the principle wavelength of the CO_2 laser [10.6 μm]. The purpose of determining the absorbance at the interface of the SU8 and the substrate is to find out the refluxing heat that gets reflected at the interface and not transmitted conductively to the sides which would aid in melting of the interface and in general promoting adherence of the SU8 micro-drop over Si/glass substrate [27]. Intuitively, one

would assume glass to offer higher reflectivity and greater refluxing of the heat to the interface with minimum conductive loss. Quantitatively the absorbance can be obtained from Eq. (6).

$$\varepsilon = \frac{N_A \cdot Absorptioncrosssection}{1000 \cdot \ln(10)} \tag{6}$$

where, N_A is Avogadro no. representing number of constituent particles per mole of a given substance and the absorption cross section will be assumed to be in cm^2 [28]. The absorption cross section is considered to be in terms of the laser beam spot-size on the exposed substrate. The spot-size is imaged and measured using Nikon epifluorescence microscope. Calculation of the Droplet Volume is explained in Supplementary Section1 (a).

Results and Discussions

Optimization of Machining Parameters

Table 1 shows the strength of the laser welding process qualitatively with respect to the power/ speed percentage of maximum values. The maximum power of the laser source is around 32 W and the maximum speed is 15.4 cm/sec. Desired strength of the laser welded fiber bond was obtained with the parameters mentioned in row 2–5 while poor weld strength was obtained at row no. 1. Out of all the different parameters; experiments show that a combination of 50 % power and 1 % speed corresponds to the best bonding between the fiber, SU8 photo-resist and the silicon substrate and it also corresponds to highest transmittance. We hypothesize that if the fiber is very well bonded then the transmittance is also higher as the DOE module is tuned between getting the optimum machining conditions resulting in delivering greatest transmittance %. Contour plot output from the DOE is provided in Fig. 4. It predicts the maximum transmittance level corresponding to 72 % obtained at Laser power of 52.90 % of maximum power and speed corresponding to 1 % of maximum speed which is very close to the actual values at which the bond strength of the joint is very good as illustrated in Table 1 reported earlier. Therefore, it is concluded that there is a very high level of correlation between the transmittance % and good bonding strength. The actual transmittance % experimentally observed is actually 2 % higher than the DOE predicted value which may be improved by taking more no. of observations in the model.

Results of COMSOL Simulations for Predicting the Heat Transfer of Laser Assisted Fabrication

Simulation of the laser heat transmission process used for welding between fibers by using SU8 micro-droplet has shown a temporal variation in temperature distribution of the laser exposed area. The heat is rapidly dissipated across the micro-droplet as well as the surface. As detailed earlier the heated substrate is responsible for refluxing back the heat to the SU8 layer along the interface if it is a poor heat conductor. In fact due to the rapid temperature rise and a cross-over of the ‘Tg’ value of uncross-linked SU8 2025

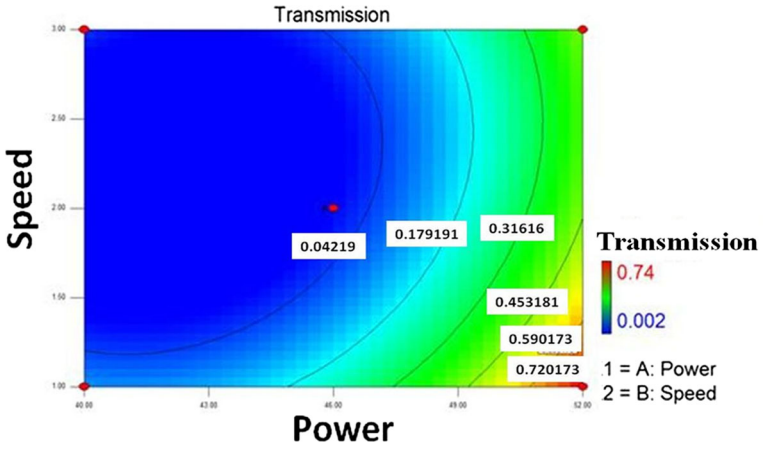

Fig. 4 Shows the design of experiments results indicating the transmission as output with speed and power

(50–65 °C); the melt pool gets formulated and is superheated near the interface due to the heat refluxing action of the substrate [29]. This is clear in the simulation output which is reported in Fig. 5.

The temperature starts to rise as the Laser is coupled at time instant '0' to the micro-droplet and simultaneously heat transfer processes occur so that equilibrium is achieved in around 125 milliseconds. The equilibrating temperature is shown as 560 K (287 °C) which is 1 μm away from the interface [based on sectional plot in supplementary figure S3] and the temperature further decreases away from the interface towards the bulk of the SU8 material. In fact at distance 10 μm from the interface the temperature is 470 K [197 °C]. Thus very near to the Si surface

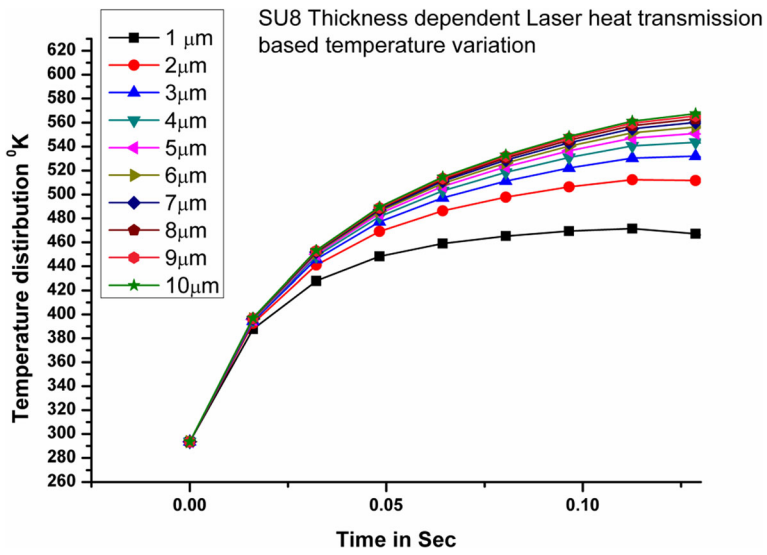

Fig. 5 The simulation output of bulk temperature of SU8-2025 vs. time of heat treatment. [Different plots show the temperature behavior from a surface 10 μm above the interface in the SU8 layer treated as 'zero datum' towards the interface]

although the temperature reaches the melting point of SU8 it does not go into the decomposition temperature for SU8 which is about 380 °C [30]. The glass being a higher reflector of incident beam may actually shoot up to above 380 °C which may degrade the SU8 because of very less absorbance of the substrate on beam incident side. So, we can see that as the laser processing involves similar conditions of the laser power, scan rate, laser frequency and resolution as obtained in the earlier section the exposed zone is always having a molten state which solidifies as soon as the Laser power is decoupled. The interface therefore is ideal to the placement of the input/ output fibers and a stronger joint formulates as the fibers are aligned or misaligned as per Fig. 1 on the surface of the substrate (interface of SU8 and substrate). The model also accounts for the conductivity of the wafer and if the conductivity resulting in interfacial heat loss is considered then the overall maximum temperatures achieved at the interface should be lower for Silicon substrate. It is due to higher thermal conductivity of silicon than glass.

As the micro-droplet is heated the reflux always tends to create a layer of molten SU8 which may be very small over the whole interface of SU8/ Si. This is true although the actual exposure area of SU8 to laser is smaller than the overall drop dimensions. The melting; that may be happening away from the hot spot is probably due to heat reflux but this melting may only be limited to a region very close to the substrate surface. Beyond this region there may be a possibility that the state has semi solid nature. The birefringence estimation is performed starting from the interface to the bulk of the droplet and obviously the superheated molten state of SU8 that is formulated closer to the interface will have more refractive index homogeneity thus causing less amount of birefringence. As the distance from surface is increased then away from the hot zone as the SU8 may still be semi solid there may be large variation of refractive index causing an increase in the overall birefringence. Simulated effective birefringence data is plotted for SU8/Si combination. [See Fig. 6].

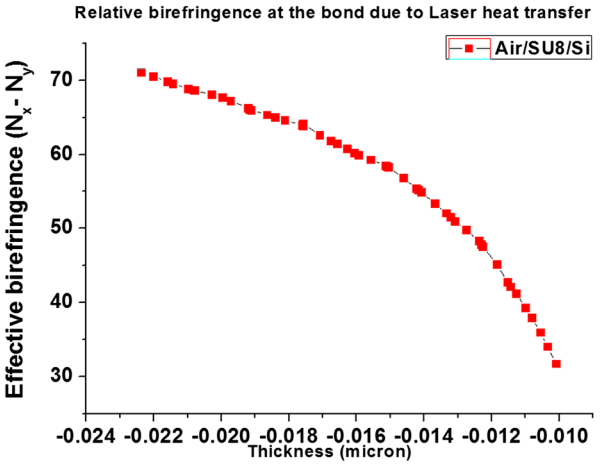

Fig. 6 Simulated estimation of effective bi-refringence with respect to distance from the surface for Air/SU8/Si combination. The formulation of a small interfacial liquid layer due to heat reflux also accounts for the fact that the bonding is substantially improved as this layer resolidifies

Simulation Results of WGM Modelling

Two different aspects are studied in this module corresponding to the aligned and misaligned cases as detailed in Fig. 1 earlier. In the aligned case the input and output fibers are aligned axially and the distance between them is varied from 1 ~ 5.5 μm. The geometry constructed while simulating in COMSOL that demonstrates the WGM effect most prominently happens for an ellipsoidal droplet [31] having a diameter of overall 6.0 μm along the major axis and 4.0 along the minor axis and therefore we have used the same with a refractive index 1.67 at the boundary of the SU8 and a refractive index 1.46 of optical fiber for performing our simulations. The fibers in the aligned case are first separated through a distance of 5.5 μm to capture the WGM based transmission of optical power. This is followed by a gradual movement of the output fiber towards the input fiber (spatially fixed) upto an extent where the fiber can almost touch each other. The transmissibility of the input signal in all these cases are simulated and Fig. 7a ~ h show output of such simulations.

A similar study is conducted with the misaligned case where the fibers are separated perpendicularly to their axes. The fibers are initially positioned tangentially to the ellipsoidal micro-droplet configuration and later manoeuvred in a similar manner with

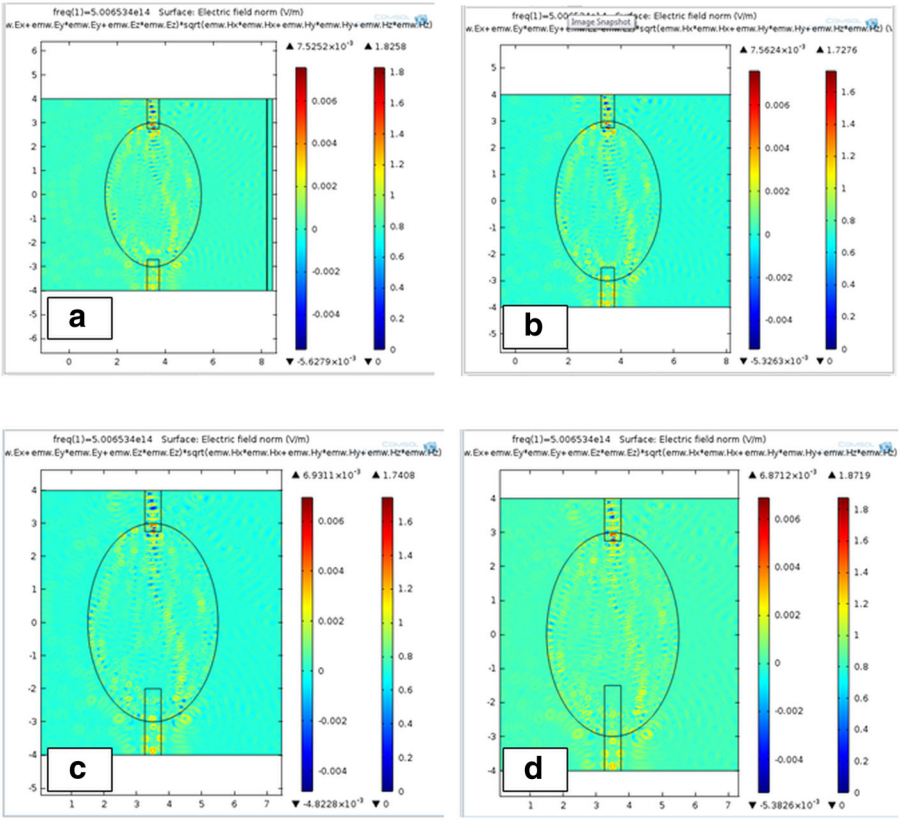

Fig. 7 Simulation output of the aligned case with inter-fiber distance **a** 5.5 μm **b** 5.3 μm **c** 4.8 μm **d** 4.3 μm **e** 3 μm **f** 2 μm **g** 1 μm and **h** 0.1 μm

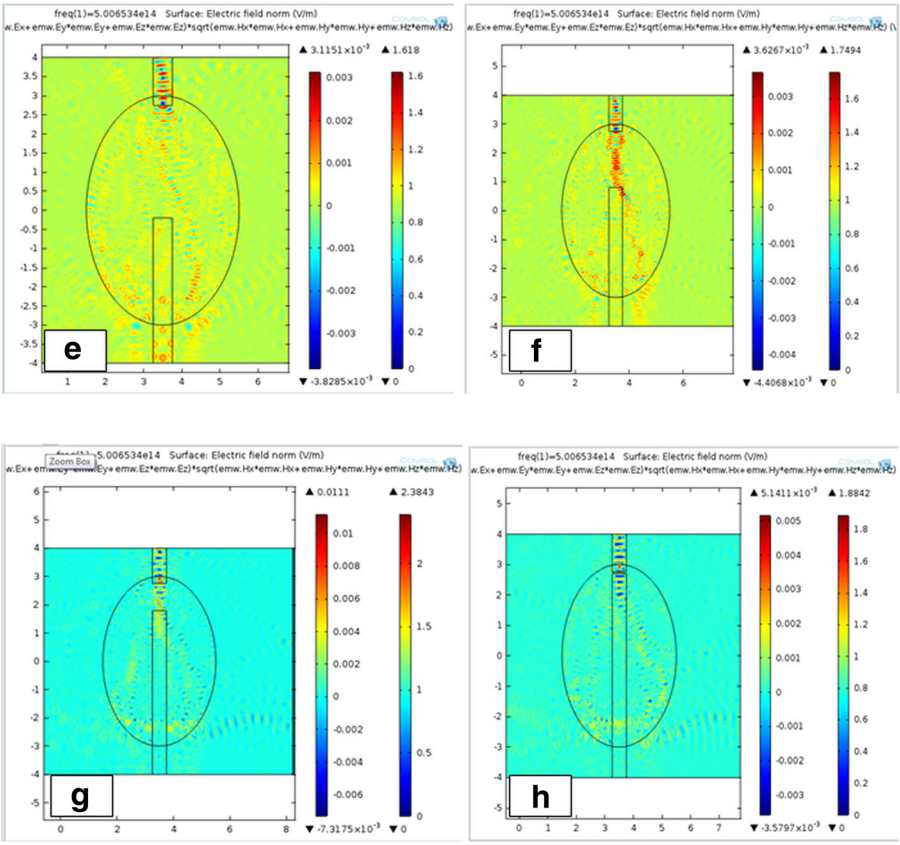

Fig. 7 continued.

input fiber fixed and the output fiber varying radially inwards. The simulation for the same are recorded as supplementary figure S4 (a)~(f). Figure 8 shows a bar graph with the various simulation predicted transmittance % corresponding to Fig. 7.

The predicted simulation output in the aligned case shows that as the inter-fiber distance approaches the diameter of the micro-droplet there is a tremendous increase in transmittance % between the input and output fibers (almost to the extent of 100 %). At other distances of separation the overall transmittance is lower than 45 % owing to scattering effects of the micro-droplet material etc. Similarly, in the misaligned case the maximum % transmittance of 65 occurs at an inter-fiber distance of 2.0 μm. This separation distance brings both the fibers close to the circumference of the ellipse as indicated in supplementary figure S4 (e) and (f). Therefore, through simulation prediction it appears that as the inter-fiber spacing is rhymed with the WGM zone in the ellipsoidal droplet there is a sudden increase in transmittance % although the fibers are misaligned and also separated by higher distances. The relative refractive index of the SU8 with respect to the fiber material is also a critical question in determining the coupling efficiency between the SU8 and the fiber at the interface. For sake of ruling out this refractive index contrast as a mechanism to reduce coupling efficiency we have

tried to find out the acceptance angle at the fiber SU8 interface and we see that the acceptance angle for the fiber air interface and that of the fiber SU8 interface are not heavily displaced. In fact the acceptance angle of the fiber air is less than that of the fiber SU8. [Please refer to supplementary section 2].

Experimental Measurement of Optical Transmittance

We have used the setup described earlier in Fig. 3 for measuring the % transmittance through the mathematical relationship expressed in Eq. 2. The transmittance study is

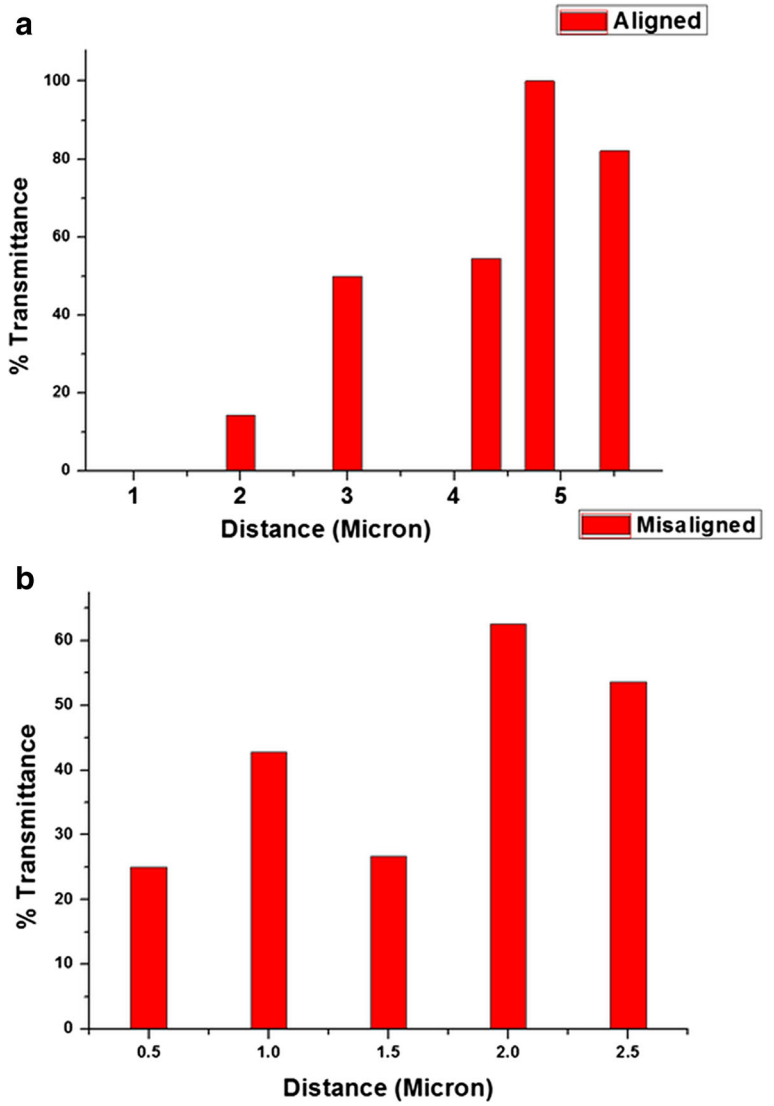

Fig. 8 Simulation predicted % Transmittance with respect to inter-fiber distance for **a** Aligned fiber and **b** Misaligned fiber cases

performed for both the aligned and misaligned cases identical to that predicted by simulations. In this case the micro-drop diameter is more realistic and in the range of 1130 μm as shown in the optical micrograph reported earlier in Fig. 2b. The inter-fiber distance in the aligned fiber case is varied from '0' to 650-microns. The fiber diameter itself is around 125 μm and the inter-fiber distance is added to the individual fiber diameter to obtain the confinement distance. The confinement distance for both the fibers in the largest separation case comes out to be similar to the drop diameter which illustrates the possibility of coupling of optical signal through WGM effect. The transmitted intensity is recorded with wavelength and acquired digitally with the ocean optics spectrophotometer. Figure 9a and b shows two graphs of real recordings done using the spectrophotometer and acquired with spectra-suit software as detailed above in "Fabrication of optical interconnects between standalone fibers and patterned waveguides" section]. Modeling the heat transfer due to Laser heating is explained in supplementary section 1.(b).

It is seen that the highest transmittance happens pertaining to either a contact condition or if both fibers are near to the outer walls where the transmission utilizes the WGM effect. The ~80 % transmission happens in case of aligned fibers as they are butted end to end within the microdroplet. Full 100 % transmission does not happen owing to polishing defects, which is also a cause of the small 10 μm distance across the ends of the fibers. The transmission % increase as the faces of both fibers are brought near the surface of the droplet. In this condition the WGM effect pre-dominates the transmission and the transmissibility starts increasing to almost 60 % corresponding to an inter-fiber distance of 650 μm. A similar observation is recorded in the misaligned case where the maximum transmittance of 95 % is again observed as the two fibers are shifted along a direction perpendicular to the axes of both fibers upto a distance of 700 μm. This is counter-intuitive looking at the data in the aligned case. As the aligned fibers only transmit upto an extent of 60 % for separation distance 650 μm, (equivalent to a confinement distance of approximately the drop diameter) in the misaligned case due to tangential placement of the fiber ends to the WGM zone, the coupling efficiency is a lot better approximately 95 % corresponding to a separation distance of 700 μm. In the other extremity as the fibers are laterally misaligned by 10 μm the transmissibility is 80 %. The reason for this small transmissibility is again attributed to scattering of light by micro-droplet. All measurement of transmissibility are acquired through a setup

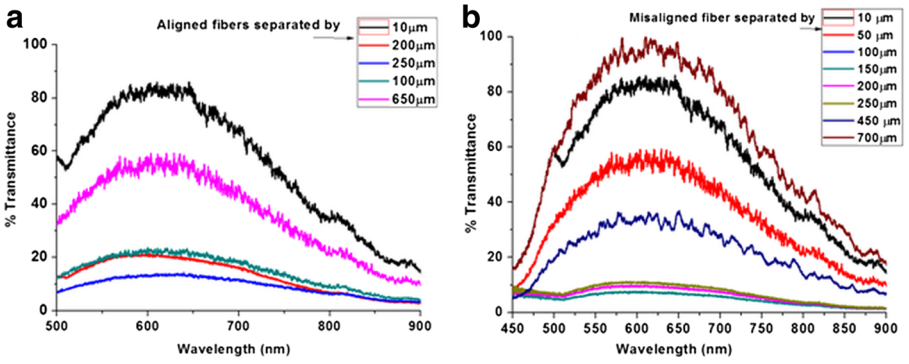

Fig. 9 Acquired data through spectra suite software using ocean optics spectrophotometer for **a** Aligned fibers **b** Misaligned fibers

illustrated in Supplementary figure S5. Therefore, the micro-droplet method using SU8 photo-resist followed by laser machining shown in the above work ideally offers a good methodology for optical tagging and joining of standalone optical fibers to furnish high transmittance even if the fibers are in misaligned orientation.

Conclusion

We have developed a new technique to tag optical fibers on the surface of a substrate by the use of SU8 which is laser exposed. The method suggested can be translated for a range of photo-patternable polymers which may have different absorption spectra. The exposure parameters of the laser source are optimized in a manner so that the SU8 very close to the substrate can melt locally upto several layers due to heat reflux from the surface of the substrate. This melt then resolidifies to ensure a good tag between the fibers, droplet and the surface. It is further ensured through heat transfer simulations that the fiber or SU8 are not degraded while getting molten. The stitched optical fiber is then extensively evaluated for transmissibility of input light to the output fiber and it is observed through simulations as well as experiments that the fibers demonstrate high transmissibility in two circumstances. One is in which the fiber is completely butted end to end and in the other configuration the fiber ends are shifted away from each other till they come very close to the outer surface of the drop where due to the WGM effect the transmissibility is again found to increase. The method has further been evaluated for two cases in which there is axial alignment between the fibers in one case and lateral shifting perpendicular to the axial direction in another case. Transmissibility is found to posses similar behaviour in both the cases. Thus the work ascertains that laser processed SU8 micro-droplet can be used to efficiently couple two or more optical fibers maintaining an overall high level of optical coupling efficiency.

Acknowledgments Authors gratefully acknowledge regular help from the 4i lab (Sh. Virendra Singh and team) at IIT-Kanpur for fabrication support and the Nano-sciences centre at IIT Kanpur for offering characterization support, the NPMASS sponsored MEMS design center (ADA/ME/20080359) at IIT Kanpur and the computer center at MNIT Jaipur for providing COMSOL Multiphysics Simulation platforms. Authors would also like to gratefully acknowledge the quality improvement program (QIP-POLY) of AICTE of the government of India, the national program on micro and smart structures (NPMASS) and MNIT Jaipur for providing the necessary financial support for this activity.

References

1. Chen, Z., Taflove, A.: Highly efficient optical coupling and transport phenomena in chains of dielectric microspheres. Opt. Lett. **31**(3) (2006)
2. Huang, S.H., Tseng, F.G.: Development of a monolithic total internal reflection-based biochip utilizing a microprism array for fluorescence sensing. J. Micromech. Micro eng. **15**, 2235–2242 (2005)
3. Yariv, A.: Critical coupling and its control in optical waveguide-ring resonator systems. IEEE Photon. Technol. Lett. **14**(4) (2002)
4. Friberg, S.R., Smith, P.W.: Nonlinear optical glasses for ultrafast optical switches. IEEE J. Quantum Electron. **Qe-23**(12) (1987)
5. Yamada, H.: Analysis of optical coupling for SOI waveguides. Piers Online **6**(2), 165 (2010)
6. Pennings, E., Khoe, G-D, Smit, M. K., Staring, T.: Integrated - optic versus Microoptic devices for Fiber-optic telecommunication systems: a comparison. IEEE J. Sel. Top. Quantum Electron. **2**(2) (1996)

7. Kuswandi, B., Nuriman, Huskens, J., Verboom, W.: Optical sensing systems for microfluidic devices: a review. Anal. Chim. Acta **60**, 141–155 (2007)
8. Tang, L., Ren, Y., Hong, B., Kang, K.A.: Fluorphore - mediated, fiber-optic, multianalyte , immunosensing system for rapid diagnosis and prognosis of cardiovascular diseases. SPIE J. Biomed. Opt. **11**(2) (2006)
9. Mehrabani, S., Maker, A.J., Armani, A.M.: Hybrid integrated label - free chemical and biological sensors. Sensors **14**, 5890–5928 (2014)
10. Wang, Chocat, N.: Fiber-optic technologies in laser-based therapeutics: threads for a cure. Curr. Pharm. Biotechnol. **11**(4), 384–397 (2010)
11. Moore, G.E.: Lithography and the future of Moore's law. Proc. SPIE 2440, Optical/Laser Microlithography VIII **2** (1995)
12. Helebrant, Buerhop, C., Weiβmann, R.: Mathematical modelling of temper$_a$ture distribution during CO2 laser irradiation of glass. Glass Technol. (1993)
13. Casalino, G., Ghorbel, E.: Numerical model of CO2 laser welding of thermoplastic polymers. **207**(1–3), 63–71 (2008)
14. Shuja, S.Z., Yibas, B.S., Momin, O.: Laser heating of a moving slab: influence of laser intensity and scanning speed on temperature field and melt size. Opt. Lasers Eng. **49** (2011)
15. Acherjee, B., Kaur, A., Mitra, S., Misra, D.: Finite element simulation of laser transmission welding of dissimilar materials between Polyvinylidene fluoride and titanium. Int. J. Eng. Sci. Technol. (2010)
16. Melai, J., Salm, C., Smith, S., Visschen, J., Schmitz, J.: The electrical conduction and dielectric strength of SU8. J. Micromech. Microeng. (2009)
17. Rekhviashvili, S.S., Gavasheli, D.S.: Modeling of laser pulse heating of solid dielectric with a fractal structure. Am. J. Condens. Matter Phys. **2**(2), 53–56 (2012)
18. Ilie, M., Cicala, E., Grevey, D., Maltei, S., Stoica, V.: Diode laser welding of ABS: experiments and process modeling. Opt. Laser Technol. **41**(5), 608–614 (2009)
19. Aden, M., Roesner, A., Olowinsky, A.: Optical characterization of polycarbonate: influence of additives on optical properties. J. Polym. Sci. B Polym. Phys. **48**, 451–455 (2010)
20. Ho, C.Y., Wen, M-Y, Ma, C.: Computer simulation for laser welding of thermoplastic polymers. Int. Conf. Comput. Eng. Appl. (2010)
21. Wilkes, C. E.: PVC Handbook. Hanser Verlag (2005), ISBN 1-56990-379-4
22. Grove, N.R., Kohl, P.A., Allen, S.A.B., Jayaraman, S., Shick, R.: Functionalized polynorbornene dielectric polymers: adhesion and mechanical properties. J. Polym. Sci. B Polym. Phys. **37**(21), 3003–3010 (1999)
23. Tai, C.Y., Unal, B., Wilkinson, J.S., Ghanem, M.A., Barlett, P.N.: Optical coupling between a self assembled microsphere grating and rib waveguide. Appl. Phys. Lett. **84**(18) (2004)
24. Fidelia, T.: Evaluation of optical solder for fiber-to-waveguide coupling in silicon photonics. http://hdl.handle.net/1721.1/45352
25. Nguyen, V., Montalbo, T., Manolatou, C., Agarwal, A., C-y, H., Yasaitis, J., Kimerling, L.C., Michel, J.: Silicon based highly efficient fiber to waveguide coupling for high index contrast systems. Appl. Phys. Lett. **88**, 081112 (2006)
26. Feng, S., Zhang, X., Wang, H., Xin, M., Lu, Z.: Fiber coupled waveguide grating structures. Appl. Phys. Lett. **96**, 133101 (2010)
27. McMasters, D., Gillette, M.L.: Approximating Avogadro's number using glass beads and monomolecular film. Chemical education Resources Inc
28. Semenov, S.V., Yevdokimov, Y.M.: Circular dichroism of DNA liquid-crystalline dispersion particles. Biophysics **60**(2), 188–196 (2015)
29. Blanco, F.J., Agirregabiria, M., Garcia, J., Berganzo, J., Tijero, M., Arroyo, M.T., Ruano, J.M., Aramburu, I., Mayora, K.: Novel three-dimensional embedded SU-8 microchannels fabricated using a low temperature full wafer adhesive bonding. J. Micromech. Microeng. **14**(7), 1047 (2004)
30. Feng, R., Farris, R.J.: Influence of processing conditions on the thermal and mechanical properties of SU8 negative photoresist coatings. J. Micromech. Microeng. **13**(1), 80 (2003)
31. Yardi, S., Boolchandani, D., Bhattacharya, S.: Polymer waveguide and optical fiber coupling using whispering gallery modes in an elliptical micro- sleeve. Optics in the Life Sciences Congress Technical Digest, The Optical Society (OSA) (2013)